

# A Historical Solution Clustering-Guided Robust Multi-Objective Optimization Algorithm Based on Decision Variable Assortment

Peijia Zhu<sup>1</sup>, Lanlan Kang<sup>2,1\*</sup>, Wenliang Cao<sup>3</sup>, Hongping Xiao<sup>1</sup>, and Yiyong Wang<sup>1</sup>

<sup>1</sup> School of Information Engineering, Jiangxi University of Science and Technology,  
Ganzhou 341000, China

6720230777@mail.jxust.edu.cn, 6720230785@mail.jxust.edu.cn,  
6720230870@mail.jxust.edu.cn

<sup>2</sup> School of Information Engineering, Gannan University of Science and Technology,  
Ganzhou 341000, China

victoryk11@163.com

<sup>3</sup> School of Electronic Information, Dongguan Polytechnic,  
Dongguan, Guangdong 523808, China

caowl22@163.com

*Received 12 April 2025; Revised 25 April 2025; Accepted 26 April 2025*

**Abstract.** In the field of dominance robust multi-objective optimization (MOP), how to accurately quantify the robustness of solutions under uncertainty is the challenge in the identification of dominant robust optimal solutions. This paper proposes a historical solution clustering-guided robust Multi-objective optimization algorithm based on decision variable assortment (RMOEA-HSA). It combines decision variable assortment (DVA) with historical solution clustering while introducing a dominance robustness enhancement metric (RobustDR), aiming to accurately quantify the dominance robustness by using systematic analyses of the aggregation patterns of historical solutions. Subsequently, this study develops three strategies: first, employs the aggregated performance of historical solutions to quantify the dominance robustness of individuals; second, an integrated approach combining K-neighbor clustering with an adaptive search mechanism to avoid local optima; last, a DBSCAN and cosine similarity-driven population reduction (DCPR) method for elite individual selection. Superior stability is demonstrated through nine benchmark tests against four existing state-of-the-art algorithms.

**Keywords:** robust multi-objective optimization, uncertainties, evolutionary algorithm, categorization of decision variables

## 1 Introduction

To maintain the validity and adaptability of optimization outcomes in dynamic and uncertain environments, significant research efforts have been devoted in recent years. K. Deb and H. Gupta introduced the concept of robustness into MOPs (RMOPs) and proposed two different types (Type I and Type II robust) of robust solutions [1]. In [2], the authors decomposition-based DBEA-r algorithm that incorporates Six Sigma metrics to simultaneously assess feasibility and performance robustness. In [3], the authors proposed a competitive co-evolutionary algorithm for solving robustness challenges in multi-objective optimization problems, where worst-case minimization is achieved through competition between two populations without the need to explicitly include a robustness measure in the objective function or constraints. In [4], the authors proposed a robust Gaussian process model to infer Bayesian risk criteria to quantify robustness. In [5], the authors innovatively introduced survival rate as an optimization objective, providing a new perspective for robustness quantification.

Some scholars have worked on decoupling the search processes of Pareto-optimal and robust-optimal solutions to resolve their inherent conflicts. In [6], the authors proposed region robustness detection to quantify the robustness of different search regions. In the same year, they proposed a robust optimal frontier construction strategy, which achieves a comprehensive solution quality assessment by combining a dual assessment

---

\* Corresponding Author

mechanism of survival algebra penalties and target space robustness metrics [7]. In [8], the authors have achieved targeted optimization of robust key variables through decision variable assortment and alternate optimization.

In [9], the authors proposed an evolutionary algorithm based on decision variable clustering, which extends the scalability study from the target space to the high-dimensional decision space for the first time. In [10], the authors developed the Dynamic Collaborative Co-evolutionary Algorithm (DCC/IDVCA), which evaluates the robustness contribution of the variables weighted by the historical information, and significantly reduces the computational overhead. Further, the authors in [11] used a dual-file mechanism to separate optimal from robustness selection and utilized adaptive bootstrap vectors to enhance the quality of high-dimensional solutions, while the authors in [12] improved the variable classification method by constraining the non-dominated sorted differential evolution.

At the core of current research difficulties is the intractable balance between optimality and robustness requirements. Consequently, this paper proposes a Decision Variable Assortment (DVA)-based algorithm designed to efficiently identify dominant robust optimal solutions. The key contributions of this work can be summarized as follows:

1. A new strategy called historical solution-based robustness assessment (HSRA) is proposed. This method employs the aggregated performance of historical solutions to quantify the dominant robustness of individuals, thereby incorporating the influence of superior solutions.
2. This study proposes an adaptive search strategy guided by K-nearest neighbor clustering, which enables the algorithm to: firstly identify critical topological structures in the solution space through density-based clustering analysis, and secondly, strategically generate new solutions in sparsely populated regions to effectively escape local optima.
3. Building upon the clustering framework, this paper incorporates pairwise cosine similarity measurements to systematically preserve solutions demonstrating superior RobustDR performance, while rigorously maintaining population diversity throughout the optimization process.

## 2 Related Works

### 2.1 Robust Multi-objective Optimization Problems (RMOPs)

In the literature, robust multi-objective optimization problems (RMOPs) are typically characterized by three primary forms of uncertainty, extending the conventional definition of multi-objective optimization:

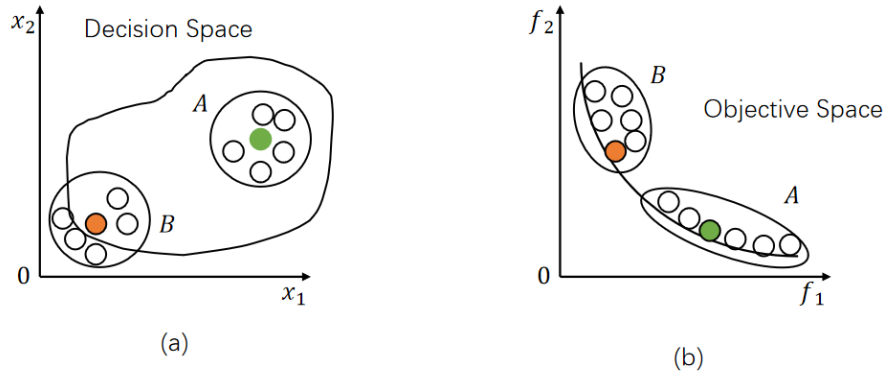
$$\begin{aligned}
& \text{minimize } F(x) = \left( f'_1(x', c'), \dots, f'_M(x', c') \right)^T \\
& \quad \text{with } x' = (x_1 + \delta_1, \dots, x_n + \delta_n)^T \\
& \quad \quad c' = (c_1 + v_1, \dots, c_k + v_k)^T \\
& \quad f'_{1:M}(x', c') = f_{1:M}(x', c') + e_{1:M} \quad \text{s.t. } x \in \Omega
\end{aligned} \tag{1}$$

In Equation (1),  $\delta = (\delta_1, \dots, \delta_n)^T$  represents the first type of uncertainty, denoting perturbations added to each decision variable. The vector  $e = (e_1, \dots, e_M)^T$  characterizes the second type of uncertainty, corresponding to evaluation noise in each objective function. Finally,  $c = (c_1, \dots, c_k)^T$  represents environmental parameters, where  $k$  denotes the number of parameters in the model. The perturbations under this uncertainty are expressed as  $v = (v_1, \dots, v_k)^T$ .

### 2.2 Dominance Robustness

**Definition 1 (Dominance Robustness, DR).** The property of a Pareto set (PS) remains within the Pareto front (PF) under slight perturbations in decision variables [13].

Definition 2 (Dominance-Robust Optimal Solution). A solution in the Pareto set (PS) that maintains its Pareto optimal and remains within the Pareto front (PF) despite perturbations in decision variables.

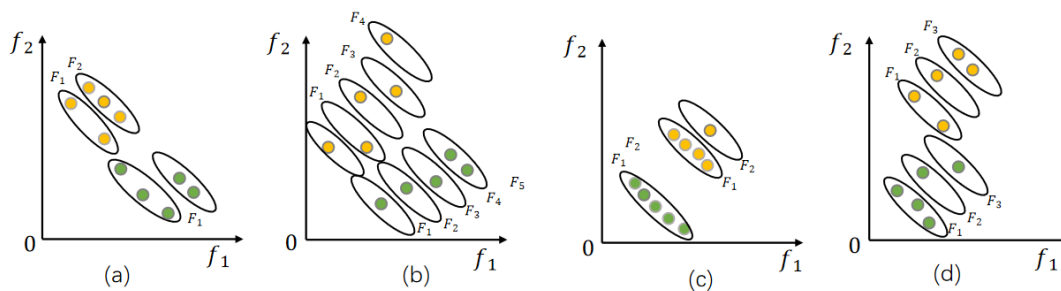


(a) The solution in decision space (b) The solution in objective space  
**Fig. 1.** Illustration of DR with a bi-objective optimization problem

Fig. 1 illustrates the concept of Dominance Robustness (DR) using a bi-objective optimization problem. Both solution A and solution B are Pareto-optimal solutions contained within the Pareto front (PF). When subjected to slight perturbations in decision variables, solution A maintains its position in the PF, while solution B may deviate from the PF due to these disturbances. This demonstrates that solution A's dominance relationship exhibits lower sensitivity to decision variable perturbations compared to solution B. Consequently, solution A possesses superior DR characteristics and can be identified as a dominance-robust optimal solution.

**2.3 Decision Variable Assortment**

Decision Variable Assortment (DVA) [8]: Since the Dominance Robustness (DR) of solutions exhibits varying sensitivity to perturbations across different decision variables, DVA classifies decision variables into Low Dominance-Robustness Variables (LDRVs) or High Dominance-Robustness Variables (HDRVs) based on their sensitivity to perturbations.



(a) Only  $x_1$  is perturbed (b) Only  $x_2$  is perturbed (c) Only  $x_3$  is perturbed (d) Only  $x_4$  is perturbed

**Fig. 2.** Illustrates how to identify LDRVs and HDRVs in a two-objective problem (In this example, there are four decision variables,  $x_1, x_2, x_3,$  and  $x_4.$ )

The core principle of DVA involves monitoring changes in solution dominance levels when decision variables are perturbed. Specifically, if a decision variable demonstrates minimal/maximal fluctuations in solution dominance levels after  $\beta$  (where  $\beta$  is set to 50) perturbation trials, it is classified as an LDRV/HDRV respectively.

The results of Fig. 2 demonstrate that  $x_3$  exhibits minimal fluctuations in dominance relationships when perturbed, qualifying it as a Low Dominance-Robustness Variable (LDRV). In contrast,  $x_1$ ,  $x_2$ , and  $x_4$  display significant sensitivity to perturbations, thereby classifying them as High Dominance-Robustness Variables (HDRVs).

### 3 A Historical Solution Clustering-Guided Robust Multi-Objective Optimization Algorithm based on Decision Variable Classification (RMOEA-HSC)

This paper proposes a novel robust multi-objective optimization algorithm incorporating historical solution clustering with decision variable analysis. The algorithm operates through three key phases:

1. Decision Variable Classification: The decision variable assortment method categorizes variables into Low Dominance-Robustness Variables (LDRVs) and High Dominance-Robustness Variables (HDRVs) for separate optimization processes.

2. LDRV Optimization: Employing non-dominated sorting and crowding distance metrics, elite solutions are selected from archive solutions [15]. To maintain archive quality, solutions exhibiting significant performance degradation are systematically eliminated from subsequent generations.

3. HDRV Optimization: the optimization of HDRVs is performed by using the historical solution-based robustness assessment to aggregate the performance of the archive solutions in place of the individual’s adaptive assessment while combining  $K$ -Neighbor clustering-guided adaptive search to identify the key structures in the solution space to avoid falling into the local optimum. Finally, DBSCAN and cosine similarity-driven population individual reduction strategy are used to identify and reduce duplicate or similar solutions to ensure the diversity of the population.

The main execution steps of RMOEA-HSC are described in Algorithm 1. The flow chart of the proposed algorithm is shown in Fig. 3.

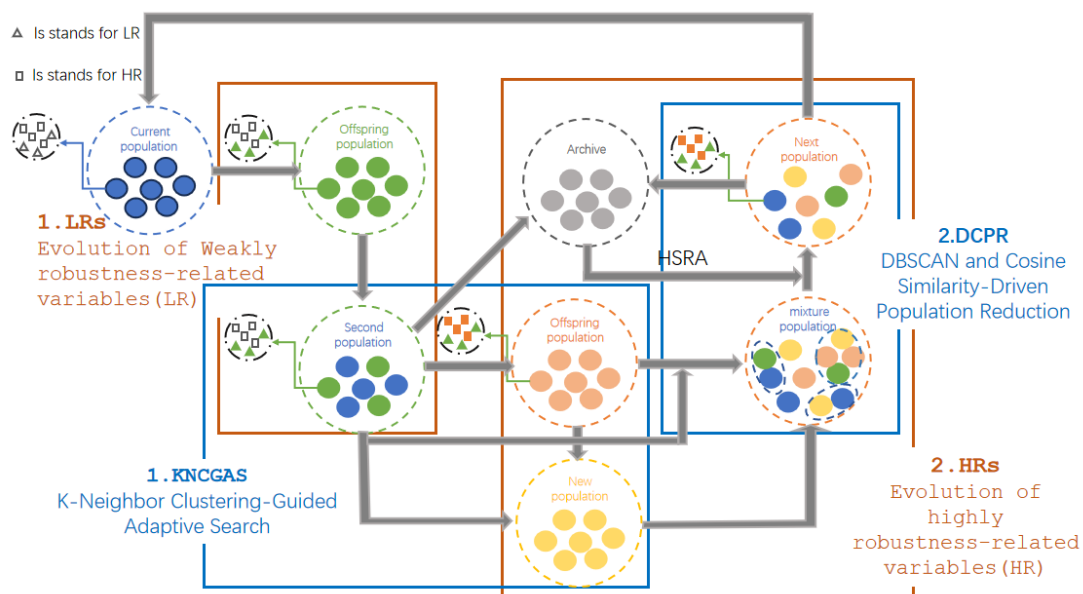


**Fig. 3.** A Historical solution clustering-guided robust multi-objective optimization algorithm based on decision variable classification with adaptive population control

**Algorithm 1.** The main steps of RMOEA-HSC

---

```

1: /* N:population size;
2: /* Population:current population;
3: /* LR:weakly robustness-related variables;
4: /* HR:highly robustness-related variables;
5: /* LRs:Non-dominant sorting and crowding distance selection for
LR;
6: /* Offspring:Cross-mutated parent generation;
7: /* PopObjX:the objective function value after perturbation;
8: /* PopDecX:the variable value after perturbation;
9: /* Archive:Elite archives from Population;
10: Initial Population;
11: Decision Variable Classification for LR and HR;
12: Population=LRS ([Population, Offspring], N);
13: NewSolution=KNCGAS ([Population, Offspring], PopObjX, PopDecX, T);
14: RobustDR=HSRA ([Population, Offspring, NewSolution], alpha, Archive);
15: Population=DCPR ([Population, Offspring, NewSolution], Problem.N);

```

---

**3.1 Historical Solution-Based Robustness Assessment**

In robust multi-objective optimization problems, accurately measuring individual robustness represents a critical strategy. Conventional dominance robustness (DR) approaches incorporate a robustness metric to quantify solution performance in the objective space, dynamically integrating this measure into fitness evaluation. While these methods employ non-dominated sorting and elite selection strategies to identify optimal populations from robust regions, their penalty functions often fail to adequately balance solution optimal and robustness when decision variables are perturbed. To address this limitation, an enhanced robustness measurement indicator is proposed.

$$PopDR(i) = \frac{\sum_{l=1}^{FNomax} (|FNo(l, i)| \times (FNo(l, i) - 1))}{H} . \quad (2)$$

This subsection presents a novel Historical Solution-based Robustness Assessment (HSRA) strategy, which introduces an innovative archive-guided mechanism. HSRA firstly maintains optimal solutions across generations while filtering out contemporary solutions exhibiting significant performance degradation, and secondly selects  $Q$  nearest archive solutions for each current individual based on Euclidean distance metrics. The robustness of each individual is then quantified through the aggregated RobustDR performance measure derived from these  $Q$ -representative archive solutions.

The dominance robustness metric  $PopDRI$  for each individual is computed using Equation (2), with the following parameters:

$H$ : the sample size is generated around individual  $i$  via Latin Hypercube Sampling (LHS).

$FNomax$ : the maximal dominance level among all sampling points in the population.

$FNo(l, i)$ : the  $l$ -th dominance level in the sampled population.

$|FNo(l, i)|$ : the corresponding number of sampling points at the  $l$ -th dominance level.

$$RobustDR(i) = \frac{PopDR(i) - \sum_{q=1}^Q Arc\_PopDR_i(q) / Q}{PopDR(i)} - 0.4 . \quad (3)$$

Subsequently, based on the Euclidean distance between individual  $i$  and archive solutions (as defined in Equation (3)), the  $Q$  nearest archive solutions to individual  $i$  are selected, where  $Q$  is set to 10.

$\sum_{q=1}^Q Arc\_PopDR_i(q) / Q$  represents the average dominance robustness metric across  $Q$  archive solutions,  $PopDR(i)$  denotes the dominance robustness metric of individual  $i$ .

The complete implementation procedure of HSRA is detailed in Algorithm 2.

---

**Algorithm 2.** HSRA

---

**Inputs:** populations, alpha, Archive

**Output:** RobustDR

```

1: Determine  $S$  from population by mini-angle elimination strategy;
2: Calculate the threshold value  $Tr$  by  $S$ ;
3: Retain individuals in the Archive whose sum of objective value is less
   than  $Tr \cdot \alpha$ ;
4: Puts  $S$  into Archive;
5: Caculate  $PopDRI$  and  $Arc\_PopDRI$  by formula 2;
6:  $Dis$ : Caculate Euclidean distances for population and Archive;
7: Select  $Q$  individuals from Archive according to  $Dis$ ;
8: Caculate RobustDR by formula 3;

```

---

### 3.2 K-Neighbor Clustering-Guided Adaptive Search

To mitigate premature convergence in local regions while preserving exploration capability and enhancing adaptability in complex dynamic environments with uncertainties, this paper introduces an adaptive search strategy guided by K-nearest neighbor clustering, whose pseudocode implementation is presented in Algorithm 3.

---

**Algorithm 3.** KNCGAS

---

```

1: Idx: Assigning cluster labels based on DBSCAN;
2: FrontNo: Perform non-dominated sorting on the population;
3: Nos=Find((Idx==-1) && (FrontNo==1));
4: For i=1 to Sum(Nos)
5:   while Remain<5
6:     Creating  $y_i$  through Perturbation of  $Nos_i$ 
7:     if  $y_i$  is a non-dominated solution for  $Nos_i$ 
8:       Add  $y_i$  to NewSolution;
9:     else
10:      if rand() < P according to formula 4
11:        Add  $y_i$  to NewSolution;
12:      end
13:    end
14:  end
15: end

```

---

The proposed strategy employs density clustering to identify critical topological structures within the solution space, thereby preventing convergence to local optima. From the unclassified noise points, non-dominated *rank-1* solutions  $Nos(Nos_1, Nos_2, \dots, Nos_m)$  are selected for perturbation-based solution generation. During this process, all newly generated non-dominated solutions are retained, while dominated solutions undergo probabilistic acceptance based on a predefined probability function. The perturbation continues until five qualified new solutions are obtained.

The mathematical formulation of the acceptance probability function is given below:

$$P = e^{-\frac{\Delta E}{T}} \quad (4)$$

with:

$$\Delta E = \sqrt{\sum_k^M (f_k(Nos_i) - f_k(y_i))^2} \quad (5)$$

Equation(5) denotes the Euclidean distance between individual  $Nos_i$  and newly generated solution  $y_i$ , where  $M$  represents the number of objective functions, and  $f(x')$  corresponds to the perturbed objective function value after disturbance.

$$T_{new} = 0.995 \times T_{current} . \quad (6)$$

Among Equation(6) the initial value of  $T$  is 1000.

### 3.3 DBSCAN and Cosine Similarity-Driven Population Reduction (DCPR)

To enhance population diversity preservation in robust multi-objective optimization, this paper develops a novel population reduction technique integrating DBSCAN clustering with cosine similarity analysis. This approach operates through three key mechanisms: firstly density-based clustering partitions the population into distinct groups, secondly, intra-cluster cosine similarity measurements identify redundant solutions, and lastly, systematic reduction maintains diversity throughout evolutionary iterations. The complete implementation is presented in Algorithm 4.

---

#### Algorithm 4. DCPR

---

```

1: Next: Perform non-dominated sorting on the population;
2: if number of Next is less than  $N$ 
3:   Idx: Assigning cluster labels based on DBSCAN;
4:   Get ClassIdx according to Idx;
ClassIdx = (ClassIdx1, ClassIdx2, ..., ClassIdxr),  $r$  is number of cluster;
5:   Calculate angle  $a_{xy}$  according to formula 7
5:   while number of ClassIdxi more than
6:     find the pair of individuals  $x$  and  $y$  with the smallest angle;
7:     if RobustDR( $x$ ) < RobustDR( $y$ )
8:       Add  $x$  to Selected;
9:     else
10:      Add  $y$  to Selected;
11:    end
12:  end
13: else
14:   Selected N-sum(Next) individuals according to the crowding distance
15: end

```

---

The proposed approach initiates with non-dominated sorting of both the current population and newly generated solutions, preferentially retaining solutions with superior non-dominated ranks (denoted as Next). When the cardinality of Next exceeds the predefined population size  $N$ , density-based clustering is applied to partition Next into distinct groups. Within each cluster, elite individuals are selected using an enhanced minimum angle elimination strategy, as detailed below:

This study integrates the minimum angle elimination method from [7, 14] to identify solution pairs requiring selection. As implemented in [7, 14], the procedure iteratively locates the solution pair with the minimal angular distance within each cluster, eliminating the inferior solution until reaching the target population size.

In the context of an  $m$ -dimensional objective space subject to decision variable perturbations, the angular separation  $\theta$  between solutions  $x$  and  $y$  is mathematically defined as the angle formed between the vector connecting  $f_k(x')$  to the reference point  $z^*$  and the vector connecting  $f_k(y')$  to  $z^*$ .

$$a_{xy} = \arccos \frac{\sum_{k=1}^M [(f_k(x') - z_k^*)(f_k(y') - z_k^*)]}{\sqrt{\sum_{k=1}^M (f_k(x') - z_k^*)^2} \sqrt{\sum_{k=1}^M (f_k(y') - z_k^*)^2}} . \quad (7)$$

Here,  $z_k^*$  represents the minimum value found thus far for objective  $k$  among all solutions, constituting the ideal point  $z^* = (z_1^*, z_2^*, \dots, z_k^*)$ . For the solution pair exhibiting the minimal angular value  $a_x^{\min} = \min_{y \in P, y \neq x} a_{xy}$  the solution with superior performance is retained. A larger  $a_x^{\min}$  indicates better diversity preservation capability of solution  $x$ .

The solution performance is evaluated using the historical solution aggregation metric RobustDR as

previously described, where a smaller RobustDR value corresponds to better solution quality and consequently higher retention probability.

## 4 Experimental Study

### 4.1 Performance Metrics

This study employs Mean Inverted Generational Distance (MIGD), Weighted Inverted Generational Distance (WIGD), Mean Hypervolume (MHV), and Weighted Hypervolume (WHV) as evaluation metrics for the following considerations [17].

MIGD serves as a fundamental metric to quantify the convergence reliability of solutions under perturbations. The MIGD is formally defined as:

$$MIGD(P, P^*) = \frac{1}{|P^*|} \sum_{v \in P^*} \min_{u \in P} \sqrt{\sum_{k=1}^M (f_k(u) - f_k(v))^2} . \quad (8)$$

Where  $P$  denotes the obtained solution set,  $P^*$  represents uniformly distributed points on the true Pareto front, and  $M$  is the number of objectives. The term  $\min_{u \in P} \|u - v\|_2$  calculates the minimal Euclidean distance from each reference point  $v \in P^*$  to the solution set  $P$ . This metric is particularly sensitive to gaps or outliers in the solution distribution.

WIGD evaluates how well the algorithm preserves solutions in critical regions (e.g., high-curvature segments or decision-preferred areas) under disturbances. The WIGD metric is expressed as:

$$WIGD(P, P^*) = \frac{1}{\sum_{v \in P^*} w(v)} \sum_{v \in P^*} w(v) \cdot \min_{u \in P} \|u - v\|_2 . \quad (9)$$

The weight function  $w(v) = 1 + \frac{\text{curvature}(v)}{\max(\text{curvature})}$  assigns higher importance to points where the Pareto front exhibits pronounced curvature changes. A reduced WIGD value confirms the algorithm's capability to maintain solutions in structurally sensitive regions despite perturbations.

MHV measures the volume of objective space dominated by the solution set  $P$  bounded by a reference point  $r$ , simultaneously evaluating convergence and diversity. A larger MHV value indicates better comprehensive performance. The metric is formulated as:

$$MHV(P) = \gamma_m \left( \bigcup_{u \in P} [u_1, r_1] \times \cdots \times \bigcup_{u \in P} [u_m, r_m] \right) . \quad (10)$$

Among Equation(10),  $\gamma_m$  denotes the Lebesgue measure in  $m$ -dimensional space, and  $r_k$  is set to  $1.1 \times \max_{u \in P^*} f_k(u)$  to ensure proper boundary definition.

WHV adapts MHV to reflect decision-maker preferences by weighting different regions of the objective space. It is defined as:

$$WHV(P) = \sum_{u \in P} w(v) \cdot \prod_{k=1}^m (r_k - f_k(u)) . \quad (11)$$

For industrial applications where certain objectives (e.g., safety constraints) take precedence, it implements an exponential weight scheme:  $w(v) = \exp(\sum_{k=1}^m \alpha_k \cdot (r_k - f_k(u)))$  with  $\alpha_k$  indicating the priority of the  $k$ -th objective.

Higher WHV values signify better alignment with predefined preferences while maintaining robustness.

## 4.2 Experimental Results and Analysis

This paper conducts comparative experiments on TP1-9 [16] between RMOEA-HSC and four state-of-the-art algorithms (CNSDEDVC [12], MOEARE [7], NSGAIIDTI [1], and RMOEADVA [8]).

The benchmark problems are designed with distinct robustness characteristics: TP1 evaluates scenarios where only partial optimal fronts exhibit robustness on convex Pareto frontiers, while TP2 and TP6 assess fully robust Pareto optimal fronts. TP3 examines partially robust optimal fronts with non-convex Pareto frontiers. TP4 features discontinuous robust regions with heterogeneous robustness levels to test algorithms' convergence capability toward distinct robust zones. In contrast, TP5 contains discontinuous regions with homogeneous robustness to evaluate convergence to different Pareto front segments. TP7-TP9 investigate multi-modal challenges involving local optimal fronts, where either entire local fronts or specific sections demonstrate robustness. Experimental results are annotated using a tri-valued notation (“+/-=”): “+” indicates RMOEA-HSC's inferior performance to the comparator, “-” signifies superiority, and “=” denotes statistical equivalence, according to the Wilcoxon rank sum test. It takes the mean and standard deviation of 30 evaluations of the indicator as a measure. Parameter settings of RMOEA-HSC are shown in Table 1.

**Table 1.** Parameter settings of RMOEA-HSC

Algorithm	Parameter settings
RMOEA-HSC	N=100, gen=200, nDVA=50, theta=0.3

**Table 2.** Results of MIGD calculations for each of the five algorithms run 30 times on the test function

Problem	CNSDEDVC	MOEARE	NSGAIIDTI	RMOEADVA	RMOEA-HSC
TP1	3.9640e-1 (4.57e-2) -	2.0018e-2 (7.06e-4) -	1.7107e-2 (1.97e-4) -	3.3958e-1 (1.81e-2) -	<b>1.6661e-2</b> <b>(3.10e-4)</b>
TP2	1.1875e+0 (3.19e-1) -	6.4132e-2 (1.34e-3) -	6.2385e-2 (5.75e-4) -	3.9718e-1 (9.96e-3) -	<b>6.1956e-2</b> <b>(2.87e-4)</b>
TP3	1.3958e+0 (7.09e-1) -	8.5882e-2 (8.71e-4) -	8.4206e-2 (2.17e-4) -	4.9985e-1 (6.18e-3) -	<b>8.4023e-2</b> <b>(1.97e-4)</b>
TP4	4.7595e-1 (1.57e-1) -	4.0643e-2 (5.58e-4) -	3.8418e-2 (2.07e-4) -	3.6787e-1 (6.48e-3) -	<b>3.8260e-2</b> <b>(2.67e-4)</b>
TP5	3.0537e-1 (7.44e-2) -	4.4338e-2 (5.33e-4) -	4.2879e-2 (2.50e-4) =	3.5608e-1 (5.58e-3) -	<b>4.2742e-2</b> <b>(2.13e-4)</b>
TP6	3.1437e+1 (1.23e+0) -	1.1023e+1 (8.20e-1) -	1.2506e+1 (1.44e+0) -	1.5641e+1 (2.82e+0) -	<b>5.8246e+0</b> <b>(1.02e+0)</b>
TP7	5.7142e+1 (1.99e+0) -	2.2904e+1 (1.72e+0) -	2.3524e+1 (2.60e+0) -	2.3449e+1 (1.82e+0) -	<b>1.2829e+1</b> <b>(2.17e+0)</b>
TP8	2.3537e+1 (2.58e+1) -	3.7970e-1 (1.99e-2) -	5.0186e-1 (5.17e-3) -	4.4837e-1 (4.62e-2) -	<b>3.0524e-1</b> <b>(2.33e-2)</b>
TP9	2.2052e+1 (1.45e+1) -	<b>2.8522e-1</b> <b>(9.02e-2) +</b>	4.0817e-1 (1.04e-1) -	4.3127e-1 (1.65e-1) -	3.1248e-1 (6.69e-2)

Table 2 presents the MIGD values obtained by the five algorithms across the TP1-TP9 benchmark problems. The comprehensive evaluation demonstrates that RMOEA-HSC achieves superior performance on TP1-TP8 compared to all competitors, while MOEARE attains the optimal MIGD value specifically on TP9. The exceptional performance of MOEARE on TP9 can be attributed to the final robust frontier construction strategy, which proves particularly effective when handling problems with partially robust Pareto fronts. In contrast, CNSDEDVC, NSGAIIDTI and RMOEADVA exhibit consistently inferior MIGD values across all

test problems when benchmarked against RMOEA-HSC. These results collectively validate that RMOEA-HSC maintains better solution distribution uniformity and convergence stability throughout the entire TP test suite compared to alternative approaches.

**Table 3.** Results of WIGD calculations for each of the five algorithms run 30 times on the test function

Problem	CNSDEDVC	MOEARE	NSGAIIDTI	RMOEADVA	RMOEA-HSC
TP1	4.4111e-1 (5.42e-2) -	3.3427e-2 (3.03e-3)=	<b>3.0858e-2</b> <b>(3.17e-3) =</b>	3.6351e-1 (1.91e-2) -	3.1990e-2 (2.88e-3)
TP2	1.3922e+0 (3.42e-1) -	1.2011e-1 (1.17e-2)=	<b>1.1819e-1</b> <b>(8.20e-3) =</b>	4.6276e-1 (3.08e-2) -	1.1992e-1 (1.08e-2)
TP3	1.5762e+0 (7.60e-1) -	1.6503e-1 (1.67e-2)=	1.6615e-1 (1.32e-2) =	5.1108e-1 (1.04e-2) -	<b>1.6224e-1</b> <b>(1.45e-2)</b>
TP4	5.6392e-1 (1.83e-1) -	7.3843e-2 (5.75e-3)-	7.0749e-2 (7.02e-3) =	3.7834e-1 (7.10e-3) -	<b>7.0033e-2</b> <b>(6.19e-3)</b>
TP5	3.7901e-1 (8.42e-2) -	7.9700e-2 (5.93e-3)=	7.8796e-2 (6.50e-3) =	3.6538e-1 (7.95e-3) -	<b>7.7951e-2</b> <b>(6.83e-3)</b>
TP6	4.6114e+1 (2.41e+0) -	2.6044e+1 (2.99e+0)-	2.7843e+1 (5.44e+0) -	3.4654e+1 (9.83e+0) -	<b>1.4889e+1</b> <b>(3.41e+0)</b>
TP7	8.2603e+1 (4.67e+0) -	5.0622e+1 (6.10e+0)-	5.0520e+1 (7.65e+0) -	5.4829e+1 (7.38e+0) -	<b>3.3461e+1</b> <b>(7.41e+0)</b>
TP8	2.9209e+1 (2.76e+1) -	9.1987e-1 (1.23e-1)-	1.1165e+0 (1.04e-1) -	1.0541e+0 (2.53e-1) -	<b>7.4778e-1</b> <b>(1.34e-1)</b>
TP9	2.8902e+1 (1.55e+1) -	7.0822e-1 (2.27e-1)=	9.5878e-1 (1.42e-1) -	1.0523e+0 (2.56e-1) -	<b>6.4855e-1</b> <b>(1.24e-1)</b>

Table 3 summarizes the Weighted Inverted Generational Distance (WIGD) values achieved by the five compared algorithms across the TP1-TP9 benchmark problems. The comparative results reveal that RMOEA-HSC demonstrates superior performance over all competing algorithms on test problems TP6-TP9 while exhibiting statistically equivalent performance to both MOEARE and NSGAIIDTI on problems TP1-TP5.

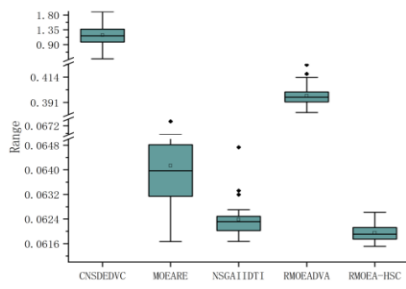
Table 4 presents the MHV comparison of five algorithms on TP1-TP9. The results show that MOEARE performs best on TP9, NSGAIIDTI achieves comparable performance to RMOEA-HSC on TP2-TP3, and RMOEADVA shows no significant difference from RMOEA-HSC on TP7. Overall, RMOEA-HSC obtains better MHV values than the other four algorithms on most problems, indicating superior comprehensive performance. Table 5 shows that RMOEA-HSC achieves the best WHV on most test problems. Fig. 4 further verifies its superior stability and convergence via MIGD distributions. Similarly, Fig. 5 demonstrates that RMOEA-HSC obtains a higher median and smaller variance in most cases, indicating better robustness than the compared algorithms.

**Table 4.** Results of MHV calculations for each of the five algorithms run 30 times on the test function

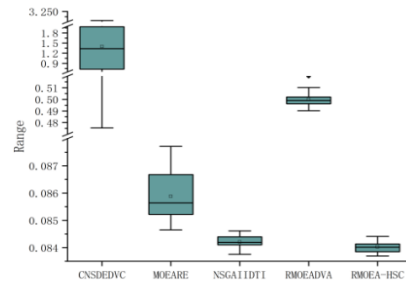
Problem	CNSDEDVC	MOEARE	NSGAIIDTI	RMOEADVA	RMOEA-HSC
TP1	2.0894e-1 (3.61e-2) -	7.0253e-1 (9.68e-4) -	7.0674e-1 (3.05e-4) -	3.0175e-1 (1.56e-2) -	<b>7.0768e-1</b> <b>(4.32e-4)</b>
TP2	2.0298e-3 (9.99e-3) -	2.6589e-1 (1.65e-3) -	2.6968e-1 (9.33e-4) =	8.4086e-2 (4.52e-3) -	<b>2.6979e-1</b> <b>(6.32e-4)</b>
TP3	1.1068e-2 (2.51e-2) -	2.4340e-1 (1.73e-3) -	<b>2.4785e-1</b> <b>(6.62e-4) =</b>	8.2920e-2 (3.84e-3) -	2.4785e-1 (7.96e-4)
TP4	1.7378e-1 (8.89e-2) -	6.0854e-1 (8.74e-4) -	6.1085e-1 (3.38e-4) -	2.7649e-1 (6.81e-3) -	<b>6.1123e-1</b> <b>(4.27e-4)</b>
TP5	2.5226e-1 (5.55e-2) -	5.2856e-1 (1.10e-3) -	5.3071e-1 (4.24e-4) -	2.1800e-1 (4.75e-3) -	<b>5.3095e-1</b> <b>(4.73e-4)</b>
TP6	0.0000e+0 (0.00e+0) -	0.0000e+0 (0.00e+0) -	0.0000e+0 (0.00e+0) -	5.3351e-6 (2.92e-5) -	<b>3.7820e-4</b> <b>(1.01e-3)</b>
TP7	0.0000e+0 (0.00e+0) =	0.0000e+0 (0.00e+0) =	0.0000e+0 (0.00e+0) =	<b>1.9962e-5</b> <b>(1.09e-4) =</b>	0.0000e+0 (0.00e+0)
TP8	1.4543e-4 (5.60e-4) -	2.8908e-1 (9.91e-3) -	2.2901e-1 (7.15e-3) -	2.5137e-1 (2.83e-2) -	<b>3.3241e-1</b> <b>(1.55e-2)</b>
TP9	0.0000e+0 (0.00e+0) -	<b>4.4709e-1</b> <b>(4.51e-2) +</b>	3.7003e-1 (5.84e-2) =	3.3829e-1 (8.32e-2) -	3.7391e-1 (9.64e-2)

**Table 5.** Results of WHV calculations for each of the five algorithms run 30 times on the test function

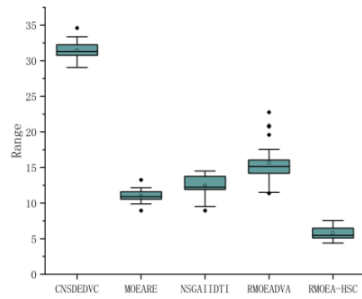
Problem	CNSDEDVC	MOEARE	NSGAIIDTI	RMOEADVA	RMOEA-HSC
TP1	1.7842e-1 (3.73e-2) -	6.8330e-1 (4.16e-3) -	6.8702e-1 (4.31e-3) =	2.8268e-1 (1.57e-2) -	<b>6.8740e-1</b> <b>(3.54e-3)</b>
TP2	0.0000e+0 (0.00e+0) -	2.1488e-1 (6.36e-3) -	2.1792e-1 (7.86e-3) =	5.4738e-2 (8.86e-3) -	<b>2.1960e-1</b> <b>(6.23e-3)</b>
TP3	6.7508e-3 (1.68e-2) -	1.9595e-1 (4.66e-3) =	<b>2.0043e-1</b> <b>(7.15e-3) =</b>	5.4701e-2 (7.90e-3) -	1.9819e-1 (7.19e-3)
TP4	1.1378e-1 (7.66e-2) -	5.7101e-1 (9.27e-3) =	5.7172e-1 (5.97e-3) =	2.6650e-1 (8.82e-3) -	<b>5.7361e-1</b> <b>(6.91e-3)</b>
TP5	1.9836e-1 (6.15e-2) -	4.8448e-1 (8.36e-3) -	<b>4.9077e-1</b> <b>(7.07e-3) =</b>	2.0908e-1 (6.27e-3) -	4.8964e-1 (7.46e-3)
TP6	0.0000e+0 (0.00e+0) =	0.0000e+0 (0.00e+0) =	0.0000e+0 (0.00e+0) =	0.0000e+0 (0.00e+0) =	0.0000e+0 (0.00e+0)
TP7	0.0000e+0 (0.00e+0) =	0.0000e+0 (0.00e+0) =	0.0000e+0 (0.00e+0) =	0.0000e+0 (0.00e+0) =	0.0000e+0 (0.00e+0)
TP8	0.0000e+0 (0.00e+0) -	1.2119e-2 (1.51e-2) -	0.0000e+0 (0.00e+0) -	1.9930e-3 (4.98e-3) -	<b>5.2933e-2</b> <b>(4.37e-2)</b>
TP9	0.0000e+0 (0.00e+0) -	<b>1.4767e-1</b> <b>(1.00e-1) =</b>	1.3954e-2 (3.01e-2) -	2.3594e-2 (3.74e-2) -	9.5931e-2 (8.78e-2)



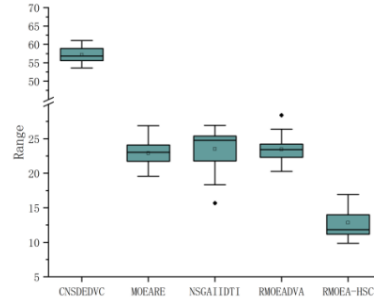
(a) MIGD on TP2



(b) MIGD on TP3

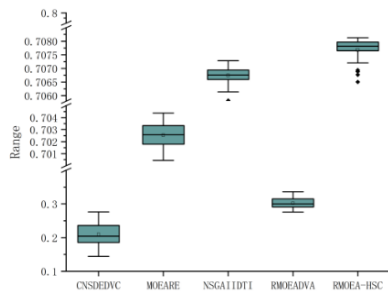


(c) MIGD on TP6

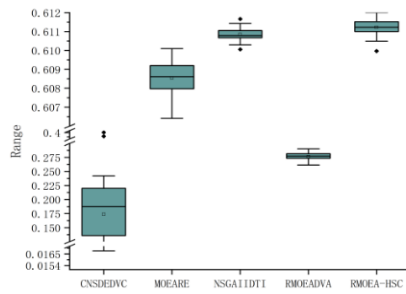


(d) MIGD on TP7

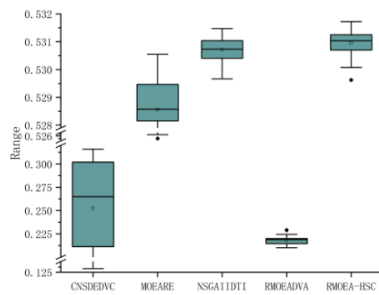
**Fig. 4.** MIGD comparison of five algorithms



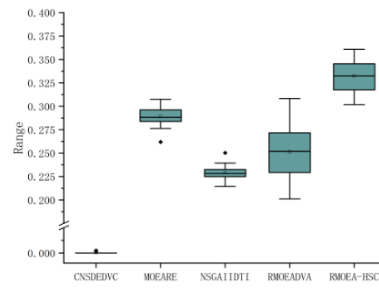
(a) MHV on TP1



(b) MHV on TP4



(c) MHV on TP5



(d) MHV on TP8

**Fig. 5.** MHV for five algorithms

### 4.3 Ablation Experiment

To validate the effectiveness of the proposed algorithmic strategies, this study conducted ablation experiments by evaluating different variants of RMOEA-HSC with specific components removed. It takes the mean and standard deviation of 30 evaluations of the indicator as a measure. Version 1 represents the algorithm without the historical solution robustness assessment strategy, while Version 2 excludes the K-nearest neighbor clustering-based adaptive search strategy.

The experimental results are evaluated using the MIGD metric, as presented in Table 6. Comparative analysis demonstrates that RMOEA-HSC outperforms its variants on eight out of nine test functions. While RMOEA-HSC demonstrated comparable mean performance to the other variants, it exhibited significantly lower standard deviation values on test problems TP3, TP4, and TP8, indicating superior solution stability. The results highlight the substantial synergistic contribution of the combined strategies to the overall algorithm improvement, emphasizing the importance of integrated strategy implementation rather than relying on any single component.

The boxplot visualization in Fig. 6 provides additional evidence, showing that RMOEA-HSC achieves more concentrated data distribution and superior stability compared to both variants.

**Table 6.** Results of MIGD calculations for each of the three algorithms run 30 times on the test function

Problem	Version 1	Version 2	RMOEA-HSC
TP1	4.3223e-2 (8.18e-3) -	1.7542e-2 (5.07e-4) -	<b>1.6661e-2</b> <b>(3.10e-4)</b>
TP2	3.5811e-1 (1.11e-2) -	6.2012e-2 (3.16e-4) =	<b>6.1956e-2</b> <b>(2.87e-4)</b>
TP3	4.5754e-1 (3.76e-2) -	8.4623e-2 (4.87e-4) -	<b>8.4023e-2</b> <b>(1.97e-4)</b>
TP4	2.9777e-1 (3.11e-2) -	3.8587e-2 (4.36e-4) -	<b>3.8260e-2</b> <b>(2.67e-4)</b>
TP5	3.1345e-1 (1.52e-2) -	4.2662e-2 (2.59e-4) =	<b>4.2742e-2</b> <b>(2.13e-4)</b>
TP6	1.5189e+1 (7.42e-1)-	8.5179e+0 (1.32e+0) -	<b>5.8246e+0</b> <b>(1.02e+0)</b>
TP7	2.6175e+1 (1.89e+0)-	2.8365e+1 (5.96e+0) =	<b>1.2829e+1</b> <b>(2.17e+0)</b>
TP8	5.8354e-1 (6.18e-2)-	3.9697e-1 (4.62e-2) -	<b>3.0524e-1</b> <b>(2.33e-2)</b>
TP9	3.3054e-1 (5.03e-2)-	<b>2.6941e-1</b> <b>(5.30e-2) +</b>	3.1248e-1 (6.69e-2)

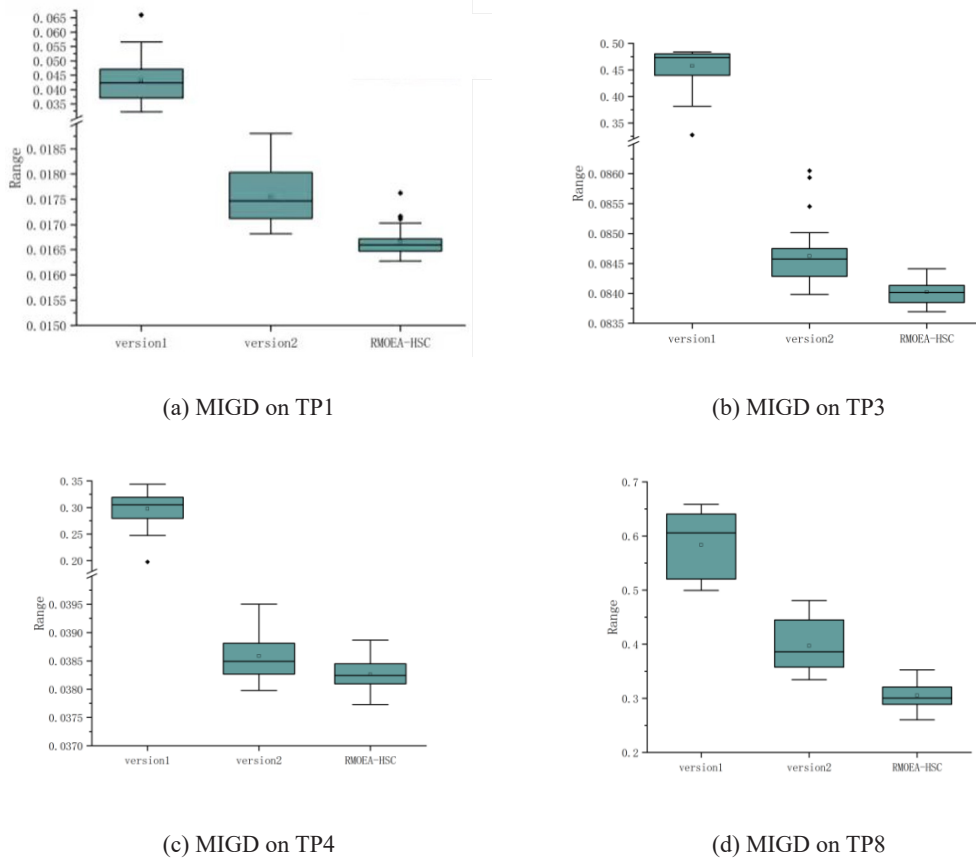


Fig. 6. MIGD for each of the three algorithms

## 5 Conclusion

This paper proposes a Robust Multi-Objective Evolutionary Algorithm guided by Historical Solution Clustering with Decision Variable Classification (RMOEA-HSC). The algorithm first classifies decision variables into High Dominance-Robustness Variables (HDRVs) and Low Dominance-Robustness Variables (LDRVs), then adopts differentiated optimization strategies to separately address optimality and robustness requirements. For LDRVs, non-dominated sorting with crowding distance selection ensures population optimal, while for HDRVs, three innovative mechanisms are implemented: (1) historical solution-based RobustDR measurement replaces individual fitness evaluation, (2)  $K$ -Neighbor Clustering-Guided Adaptive Search generates new solutions in the empty region of the objective space to avoid falling into local optima, and (3) DBSCAN and cosine similarity-driven population reduction eliminates redundant solutions to maintain diversity.

Experimental results demonstrate RMOEA-HSC's superior performance on TP problems featuring multimodality and discontinuity characteristics. However, its effectiveness diminishes when handling high-dimensional or many-objective optimization problems. Enhancing the algorithm's scalability for such complex scenarios has been identified as a critical direction for future research.

## Acknowledgement

The work of LanLan Kang was supported in part by the Natural Science Foundation of China under Grant No. 62166019, and the Natural Science Foundation of Jiangxi Province under Grant No. 20252BAC240195, and the Science and Technology Research Project in Department of Education of Jiangxi Province under Grant GJJ2403701. The work of Wenliang Cao was supported the Special for key fields of colleges and universities in Guangdong Province under Grant 2025ZDZX1084.

## References

- [1] K. Deb, H. Gupta, Introducing robustness in multi-objective optimization, *Evolutionary Computation* 14(4)(2006) 463-494.  
<https://doi.org/10.1162/evco.2006.14.4.463>
- [2] M. Asafuddoula, H.K. Singh, T. Ray, Six-sigma robust design optimization using a many-objective decomposition-based evolutionary algorithm, *IEEE Transactions on Evolutionary Computation* 19(4)(2015) 490-507.  
<https://doi.org/10.1109/TEVC.2014.2343791>
- [3] I.R. Meneghini, F.G. Guimaraes, A. Gaspar-Cunha, Competitive coevolutionary algorithm for robust multi-objective optimization: The worst case minimization, in: *Proc. 2016 IEEE Congress on Evolutionary Computation (CEC)*, 2016.  
<https://doi.org/10.1109/CEC.2016.7743846>
- [4] J.X. Qing, I. Couckuyt, T. Dhaene, A robust multi-objective Bayesian optimization framework considering input uncertainty, *Journal of Global Optimization* 86(3)(2023) 693-711.  
<https://doi.org/10.1007/s10898-022-01262-9>
- [5] W.X. Jiang, K. Gao, S.W. Zhu, L.H. Xu, A novel robust multi-objective evolutionary optimization algorithm based on surviving rate, *Complex & Intelligent Systems* 11(4)(2025) 1-25.  
<https://doi.org/10.1007/s40747-025-01822-y>
- [6] Z. He, G.G. Yen, Z. Yi, Robust multiobjective optimization via evolutionary algorithms, *IEEE Transactions on Evolutionary Computation* 23(2)(2019) 316-330.  
<https://doi.org/10.1109/TEVC.2018.2859638>
- [7] Z. He, G.G. Yen, J. Lv, Evolutionary multiobjective optimization with robustness enhancement, *IEEE Transactions on Evolutionary Computation* 24(3)(2020) 494-507.  
<https://doi.org/10.1109/TEVC.2019.2933444>
- [8] J. Liu, Y. Liu, Y. Jin, F. Li, A decision variable assortment-based evolutionary algorithm for dominance robust multiobjective optimization, *IEEE Transactions on Systems, Man, and Cybernetics: Systems* 52(5)(2022) 3360-3375.  
<https://doi.org/10.1109/TSMC.2021.3067785>
- [9] X.Y. Zhang, Y. Tian, R. Cheng, Y.C. Jin, A Decision Variable Clustering-Based Evolutionary Algorithm for Large-Scale Many-Objective Optimization, *IEEE Transactions on Evolutionary Computation* 22(1)(2018) 97-112.  
<https://doi.org/10.1109/TEVC.2016.2600642>
- [10] Y.K. Xiao, W. Du, Y. Tang, A novel implicit decision variable classification approach for high-dimensional robust multi-objective optimization in order scheduling, *Complex & Intelligent Systems* 10(3)(2024) 4119-4139.  
<https://doi.org/10.1007/s40747-024-01382-7>
- [11] S. Shao, Y. Tian, L.M. Zhang, K.C. Tan, X.Y. Zhang, An Evolutionary Algorithm for Solving Large-Scale Robust MultiObjective Optimization Problems, *IEEE Transactions on Evolutionary Computation* 29(6)(2025) 2476-2490.  
<https://doi.org/10.1109/TEVC.2024.3435006>
- [12] W. Du, W.M. Zhong, Y. Tang, W.L. Du, Y.C. Jin, High-dimensional robust multi-objective optimization for order scheduling: a decision variable classification approach, *IEEE Transactions on Industrial Informatics* 15(1)(2019) 293-304.  
<https://doi.org/10.1109/TII.2018.2836189>
- [13] L.T. Bui, H.A. Abbass, M. Barlow, A. Bender, Robustness against the decision-maker's attitude to risk in problems with conflicting objectives, *IEEE Transactions on Evolutionary Computation* 16(1)(2012) 1-19.  
<https://doi.org/10.1109/TEVC.2010.2051443>
- [14] Z. He, G.G. Yen, Many-objective evolutionary algorithms based on coordinated selection strategy, *IEEE Transactions on Evolutionary Computation* 21(2)(2017) 220-233.  
<https://doi.org/10.1109/TEVC.2016.2598687>
- [15] K. Deb, A. Pratab, S. Agrawal, T. Meyarivan, A fast and elitist multiobjective genetic algorithm: NSGA-II, *IEEE Transactions on Evolutionary Computation* 6(2)(2002) 182-197.  
<https://doi.org/10.1109/4235.996017>
- [16] A. Gaspar-Cunha, J. Ferreira, G. Recio, Evolutionary robustness analysis for multi-objective optimization: benchmark problems, *Structural and Multidisciplinary Optimization* 49(5)(2014) 771-793.  
<https://doi.org/10.1007/s00158-013-1010-x>
- [17] C.A.C. Coello, N.C. Cortés, Solving multiobjective optimization problems using an artificial immune system, *Genetic programming and evolvable machines* 6(2)(2005) 163-190.  
<https://doi.org/10.1007/s10710-005-6164-x>